

# Electrical annealing of severely deformed copper: microstructure and hardness

Saeed Nobakht and Mohsen Kazeminezhad

Department of Materials Science and Engineering, Sharif University of Technology, Azadi Avenue, Tehran, Iran  
(Received: 3 December 2016; revised: 26 February 2017; accepted: 27 February 2017)

**Abstract:** Commercial pure copper sheets were severely deformed after primary annealing to a strain magnitude of 2.32 through constrained groove pressing. After induction of an electrical current, the sheets were heated for 0.5, 1, 2, or 3 s up to maximum temperatures of 150, 200, 250, or 300°C. To compare the annealing process in the current-carrying system with that in the current-free system, four other samples were heated to 300°C at holding times of 60, 90, 120, or 150 s in a salt bath. The microstructural evolution and hardness values of the samples were then investigated. The results generally indicated that induction of an electrical current could accelerate the recrystallization process by decreasing the thermodynamic barriers for nucleation. In other words, the current effect, in addition to the thermal effect, enhanced the diffusion rate and dislocation climb velocity. During the primary stages of recrystallization, the grown nuclei of electrically annealed samples showed greater numbers and a more homogeneous distribution than those of the samples annealed in the salt bath. In the fully recrystallized condition, the grain size of electrically annealed samples was smaller than that of conventionally annealed samples. The hardness values and metallographic images obtained indicate that, unlike the conventional annealing process, which promotes restoration phenomena with increasing heating time, the electrical annealing process does not necessarily promote these phenomena. This difference is hypothesized to stem from conflicts between thermal and athermal effects during recrystallization.

**Keywords:** annealing; severe plastic deformation; copper; microstructure; hardness

## 1. Introduction

Rapid annealing can decrease the effect of recovery before recrystallization [1–2]. As recovery decreases, nucleation rates increase, the final microstructure can be refined, and the mechanical properties of the product are improved. Rapid annealing is believed to allow good microstructure control [3]. As well, if optimized conditions for annealing are applied, significant energy savings are obtained. Rapid annealing processes are carried out through salt baths, application of an electrical current, and laser exposure [4].

Rapid annealing by application of an electrical current, also called electropulsing treatment, is a novel method in which an electrical current is passed through metal; the electrical resistivity of the metal produces heat and leads to microstructural evolution [5]. In this process, a large amount of energy is imposed on the metal over a very short period of time, existing dislocations in hard-worked metal are re-

moved, and a stable energy situation is finally achieved [6]. Electropulsing treatment has attracted significant attention in the industry because of its efficiency and has been applied to various fields such as electroplasticity, powder densification, recrystallization, crack and damage healing, and medical science, among others [6–7].

Many studies concerning the effects of an electrical current on microstructural evolution have been conducted, and these works generally report that electron flows exert a direct influence on the diffusion process and dislocation mobility of a metal [7–10]. When an electrical current is passed through a metal, the electron momentum is changed from the equilibrium value  $K_0$  to the peak value  $K_{\text{Max}}$ . These findings support the concept of momentum change causing a contact force to be transmitted to atoms. Momentum change is expressed as [6,11]:

$$\Delta K = \bar{K} - \bar{K}_0 = \int_0^t F dt \quad (1)$$

where  $\vec{K}$  is the electron momentum vector,  $\vec{K}_0$  is the equilibrium electron momentum vector,  $F$  is a contact force and  $t$  is the duration of current induction. Eq. (1) indicates that, when the value of momentum change is held constant, a high contact force is maintained because of the short application of pulses during electrical annealing. This high contact force, in addition to atomic vibration, results from the heating effect, which increases the kinetic energy of atoms [6,11].

Several experiments on microstructural evolution have been carried out based on different rapid annealing methods. However, very few studies on the rapid annealing of severe plastic-deformed metal, especially through the electropulsing method, have been reported. In previous investigations, while the influences of frequency, current density, and temperature were extensively explored, the time effect was not taken into account as an independent variable during annealing. Therefore, the present study aims to obtain a better understanding of the microstructural evolutions in severely plastic-deformed copper during rapid annealing.

## 2. Experimental

### 2.1. Sheets material

In this research, commercial pure copper sheets (99.8%)

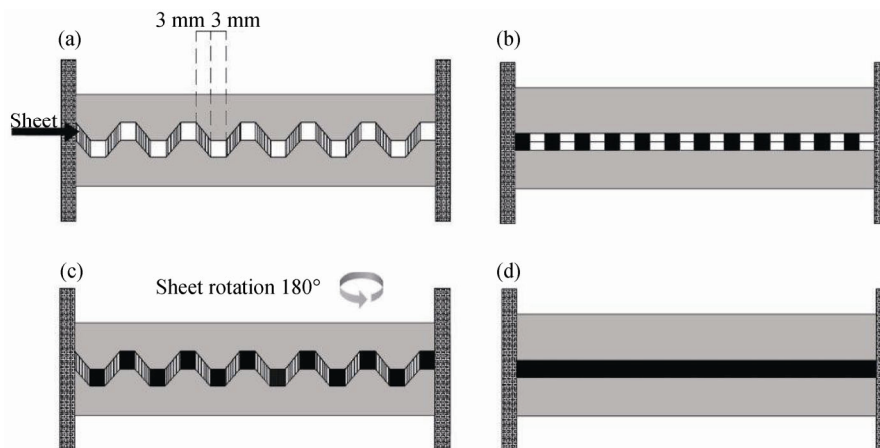


Fig. 1. Schematic of the steps of the constrained groove pressing process representing one cycle of deformation.

### 2.3. Annealing process

After two cycles of CGP, the sheets were separately annealed using an electrical annealing system or in a salt bath to investigate the effect of rapid heating on the microstructural evolution and hardness of severely deformed copper.

#### 2.3.1. Rapid annealing with an electrical current

An ultra-rapid annealing (URA) setup was designed based on “Resistance Heating” [13]. A high heating rate was provided by a high current transformer controlled by a

digital control unit [13]. The temperature was measured using an attached thermocouple from the center of the sample [13] and read at a rate of 3000 samples per second using a data-logger [13]. These data were concurrently transferred and saved to a computer, and a temperature-time diagram was plotted during URA [13]. After reaching the peak temperature, the specimen was cooled immediately by a high-speed spray of water and air [13]. Figs. 2 and 3 respectively illustrate the electrical/rapid annealing system and a temperature versus time graph of a rapidly annealed sample.

### 2.2. Deformation process

The annealed sheets subjected to two cycles of constrained groove pressing (CGP) at room temperature to achieve an equivalent strain magnitude of 2.32. Figs. 1(a)–1(d) illustrates the four steps of the CGP process forming one cycle of deformation. In the first step, the sheet was placed between two grooved surfaces of an asymmetric die and pressed in a plane-strain state; as a result, some regions of the sheet were inclined and subjected to an equivalent strain of 0.58, while other regions did not show any deformation (Fig. 1(a)). In the second step, the grooved sheet was flattened using a die and an equivalent strain of 0.58 was imposed on deformed regions once more (Fig. 1(b)). At the end of this step, a flat sheet consisting of two regions with equivalent strain of 1.16 and without strain was produced. In the third step, the sheet was vertically rotated 180° relative to the sheet plane, and the first and second steps were repeated (Figs. 1(c)–1(d)). Finally, a complete sheet with an equivalent strain of 1.16 was produced [12].

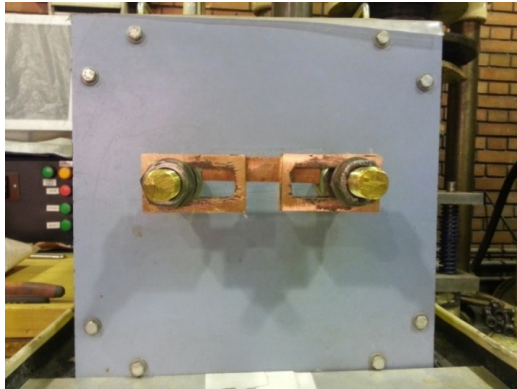


Fig. 2. Schematic of the electrical annealing system used in this work.

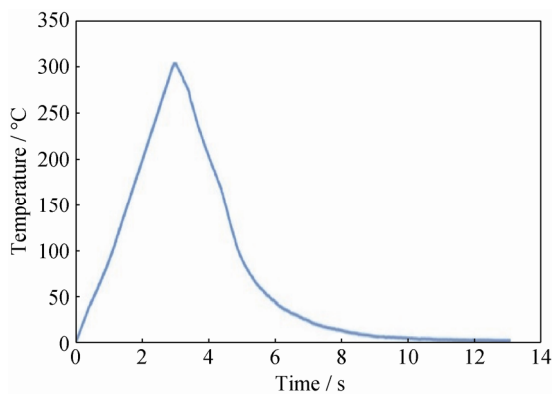


Fig. 3. Schematic of the heating process in an electrical annealing system at temperatures up to 300°C.

In this research, rapid annealing with an electrical current was performed at maximum temperatures of 150, 200, 250, or  $(300 \pm 15)^\circ\text{C}$  for heating times (i.e., the time required to reach the maximum temperature) of 0.5, 1, 2, or  $(3 \pm 0.1)$  s. All of the experiments were performed at a constant voltage (5 V) and frequency (50 Hz).

#### 2.3.2. Annealing in salt bath

To compare the results of electrically annealed samples with those of conventionally annealed samples, another set of samples was annealed in a salt bath. Annealing was performed in an AS140 salt bath at a constant temperature of

$300^\circ\text{C}$  for holding times of 60, 90, 120, or 150 s, after which the samples were cooled in water. Fig. 4 shows a schematic of the heating process in a salt bath.

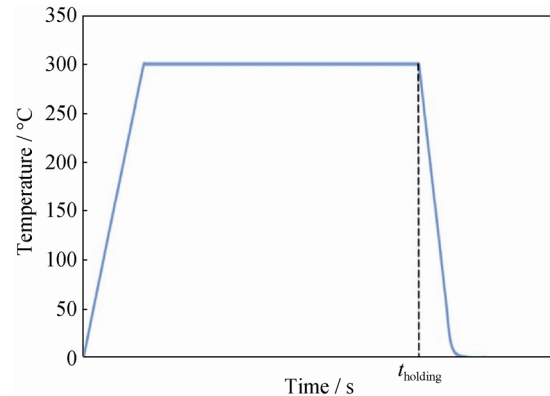


Fig. 4. Schematic of the heating process in a salt bath at a constant temperature of  $300^\circ\text{C}$ .

#### 2.4. Microstructure and hardness investigations

Metallographic examinations were carried out using an optical microscope after surface preparation and etching in a mixture of 25 mL of  $\text{H}_2\text{O}$ , 25 mL of  $\text{NH}_4\text{OH}$ , and 5 mL of  $\text{H}_2\text{O}_2$ .

To investigate the mechanical properties of the samples, a Vickers hardness test was conducted at the center of each sample. The hardness measurements were carried out with a force of 200 N. Five tests were performed and the average of these tests was considered the final hardness value.

### 3. Results

#### 3.1. Microstructure

Fig. 5(a) shows the microstructure of a primary annealed sample. Equiaxed grains may be observed. Fig. 5(b) shows the microstructure of a sample after two cycles of CGP. In this sample, the grain size is significantly decreased in comparison with that of the primary annealed sample, and a small quantity of twins may be observed.

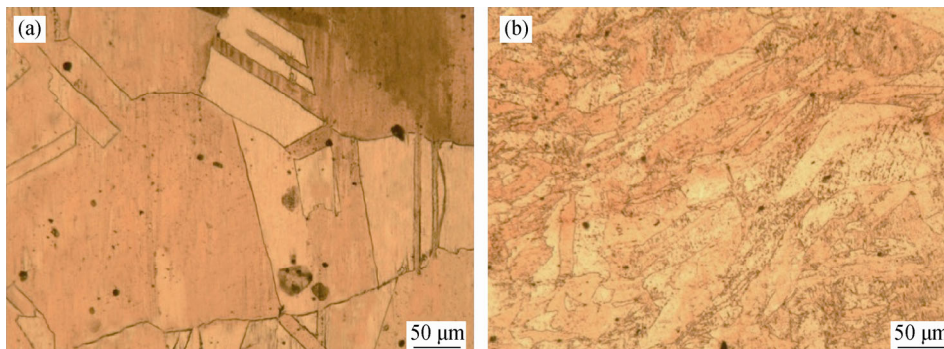
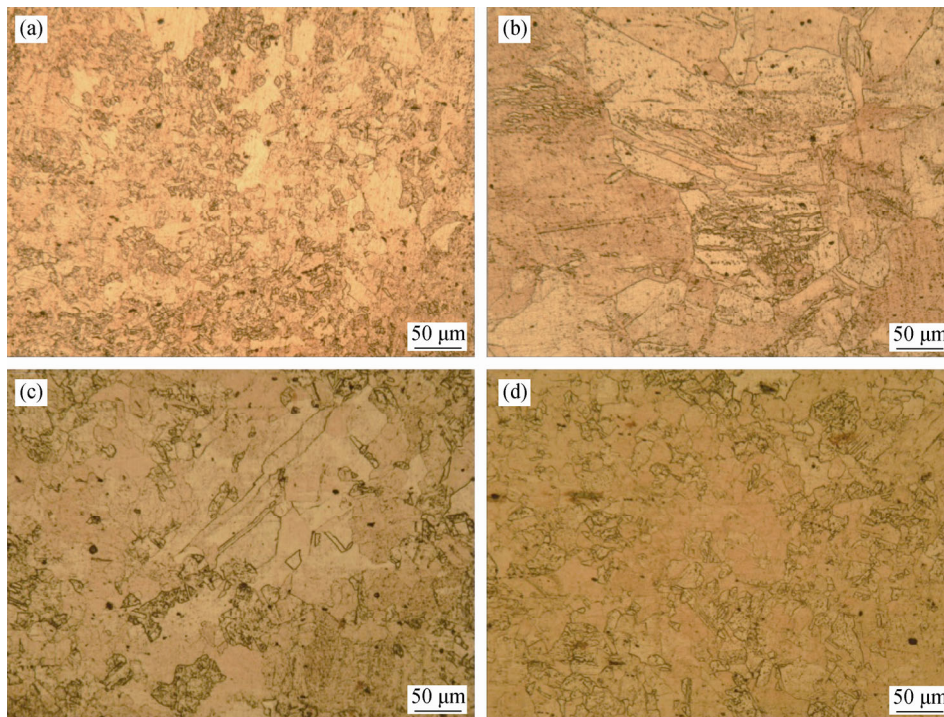


Fig. 5. Microstructures of a primary sample annealed in a furnace (a) and the sample obtained after two cycles of constrained groove pressing (b).

Fig. 6 shows the microstructure of the samples electrically annealed at a maximum temperature of 150°C for various heating times. Under these conditions, heating rates are in the range of 50 to 300°C/s. Samples heated for 0.5 s show a large number of grown nuclei resulting from recrystallization. Consequently, the microstructures of CGP samples change from the elongated state to the equiaxial state. In addition, annealing twins are observed. When the heating time is 1 s (Fig. 6(b)), recrystallized grains are not observed, but

elongated grains are clearly found. Heating times longer than 0.5 s result in unusual behavior after annealing. In Fig. 6(c), the samples heated for 2 s show a deformed microstructure, although recrystallized grains may also be observed in some regions. Moreover, as shown in Fig. 6(d), samples heated for 3 s reveal a large number of equiaxed grains (recrystallized grains). These grains are larger than those in samples heated for 0.5 s, but the distribution of recrystallized grains is fairly homogenous in both samples.



**Fig. 6.** Microstructures of the samples electrically annealed at a maximum temperature of 150°C for different heating times: (a) 0.5 s; (b) 1 s; (c) 2 s; (d) 3 s.

Fig. 7 demonstrates the microstructures of samples annealed at a maximum temperature of 200°C for various heating times. The heating rates for these samples are in the range of 65 to 400°C/s. The microstructure of the samples heated for 0.5 s (Fig. 7(a)) reveals a large number of equiaxed grains; increasing the heating time to 1 s (Fig. 7(b)) causes elongated grains to form and recrystallized grains to disappear. Increasing the heating time to 2 and 3 s (Figs. 7(c) and 7(d), respectively) causes the microstructures of the corresponding samples to develop equiaxed grains, indicating that the recrystallization process is well underway. Here, the grain sizes obtained are nearly uniform and abnormal grain growth (or secondary recrystallization) does not appear to occur.

Fig. 8 illustrates the microstructures of the samples electrically annealed at a maximum temperature of 300°C for

various heating times. The heating rates in this case are in the range of 100 to 600°C/s. Sample recrystallization appears to be well in progress and uniformly distributed equiaxed grains may be observed. The grain sizes are nearly uniform and abnormal grain growth does not take place.

Fig. 9 depicts the microstructures of the samples annealed in a salt bath at 300°C for holding times ranging from 60 to 150 s. When the CGP sample is heated in a salt bath for 60 s (Fig. 9(a)), some small recrystallized grains are formed. In this sample, grains elongated in the deformation direction are observed. When the holding time is increased to 90 s (Fig. 9(b)), the number of recrystallized grains increases and the trace of elongated grains is no longer visible. In contrast to electrically annealed samples, salt-bath annealed samples show abnormal

grain growth. As the holding time is increased to 120 and 150 s, the recrystallized grains expand and a

coarse-grain structure is achieved. Some fine grains may also be observed.

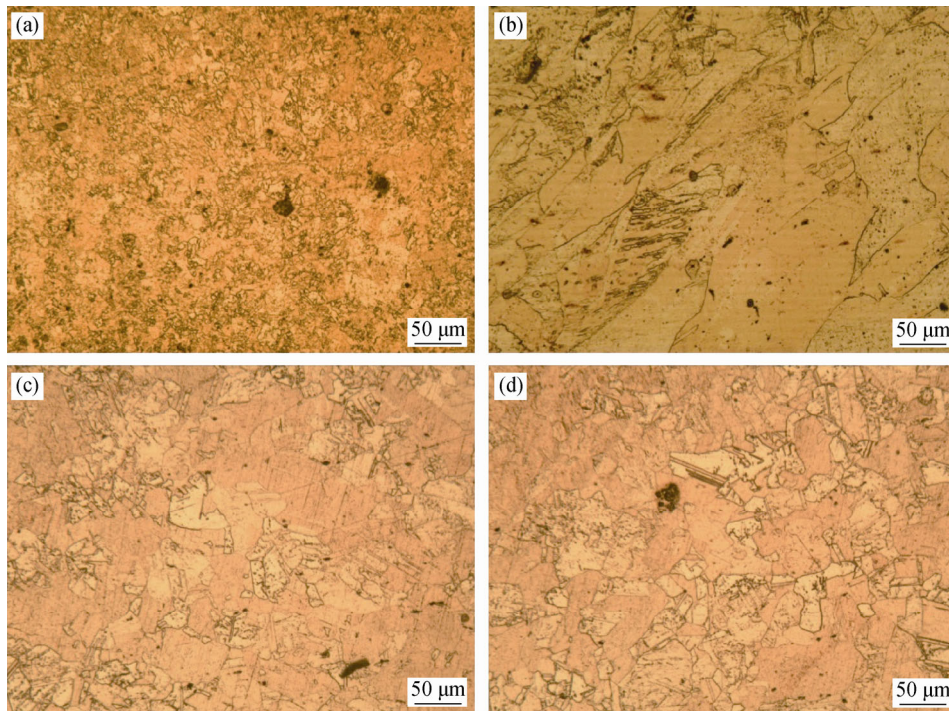


**Fig. 7.** Microstructures of the samples electrically annealed at a maximum temperature of 200°C for different heating times: (a) 0.5 s; (b) 1 s; (c) 2 s; (d) 3 s.

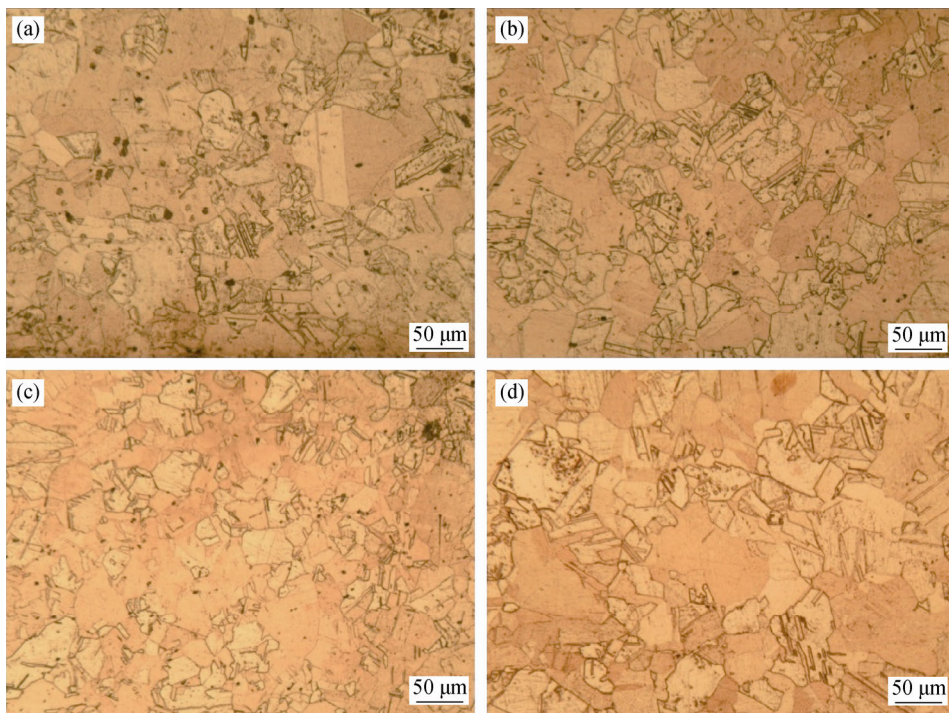


**Fig. 8.** Microstructures of the samples electrically annealed at a maximum temperature of 300 °C for different heating times: (a) 0.5 s; (b) 1 s; (c) 2 s; (d) 3 s.

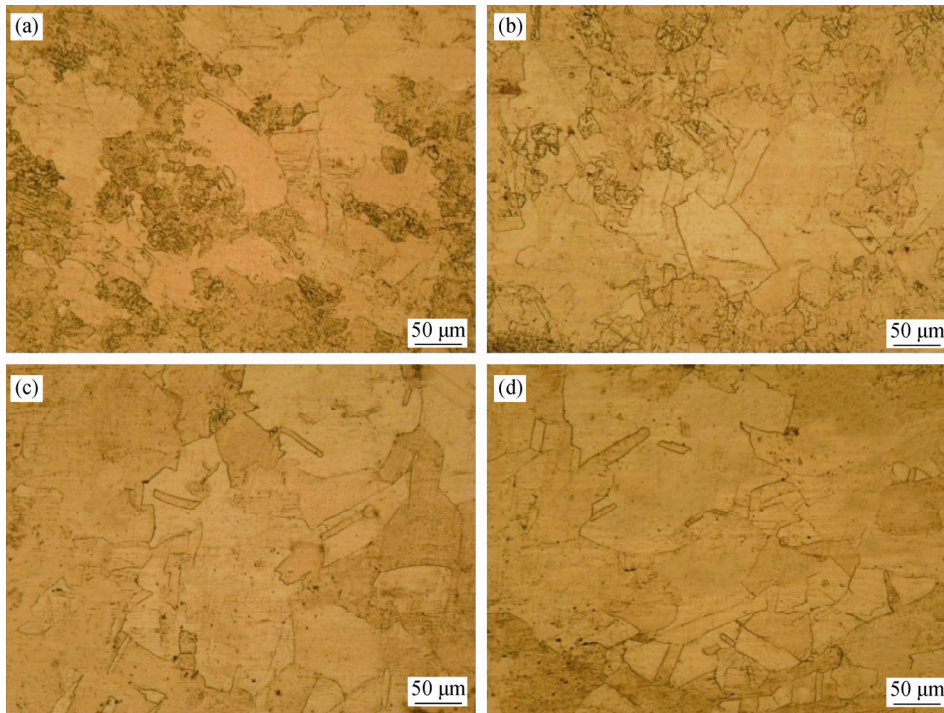


Fig. 9. Microstructures of the samples annealed in a salt bath at 300°C for different heating times: (a) 60 s; (b) 90 s; (c) 120 s; (d) 150 s.

Considering the microstructural observations, the numbers of nuclei in electrically annealed samples appear to be larger than those of conventionally annealed samples; consequently, more uniform grain sizes can be expected in the former. Unlike in the samples annealed in a salt bath, abnormal grain growth is not observed in electrically annealed samples. Interestingly, despite the higher temperature and time required for conventional annealing, the recrystallization process in this case is completed at lower rate than that in electrical annealing. This observation indicates a higher nucleation rate in the latter compared with that in the former.

### 3.2. Hardness test

Fig. 10 demonstrates the hardness test results of the as-received, primary annealed, and CGP samples. The hardness of the samples increases from Hv 31 to Hv 118 after two cycles of CGP.

The hardness test results of the samples electrically annealed under different conditions are presented in Fig. 11. Here, the hardness of the samples electrically annealed for 0.5 s at 150°C decreases from Hv 118 (in the hard-worked state) to Hv 80. When the metal is heated for 1 s at 150°C, the sample’s hardness decreases from Hv 118 to Hv 111. When the heating time is increased to 2 and 3 s, the hardness of the samples is decreased more extensively than that of the samples annealed for 1 s. These results reveal an unusual trend, i.e., the samples heated for 0.5 s show greater reductions in hardness than the samples heated for 1 and 2 s.

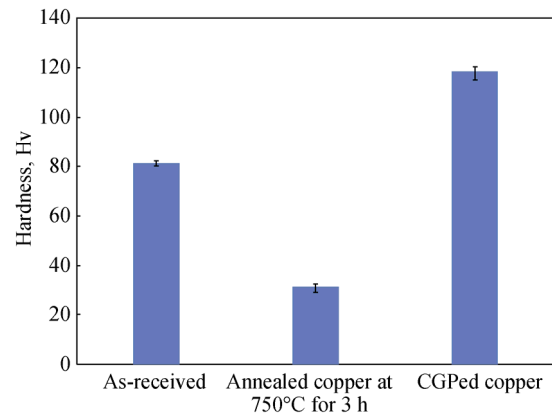


Fig. 10. Hardness of the samples at various states before electrical/rapid annealing.

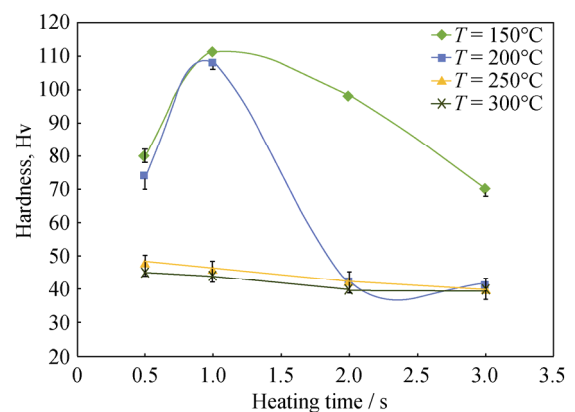


Fig. 11. Hardness of the samples electrically annealed at different final temperatures and heating times.

The unusual behavior is also observed for the heated samples at 200°C. The samples heated for 0.5 s show greater reduction in hardness than the samples heated for 1 s. When the heating time is increased to 2 and 3 s, the hardness is significantly decreased. The samples heated at 250 and 300°C show remarkable reductions in hardness for all heating times. The hardness values obtained are approximately equal to the hardness of the primary annealed sample.

Fig. 12 shows the hardness test results of the samples annealed in the salt bath. Increasing the holding time to 120 s clearly results in a sharp decrease in hardness, but increasing the holding time from 120 to 150 s shows insignificant hardness changes.

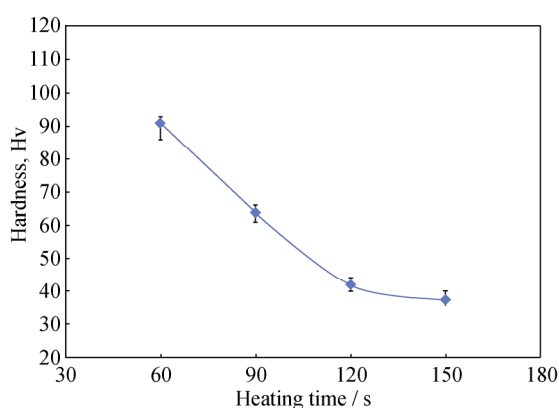


Fig. 12. Hardness of the samples annealed in a salt bath at 300°C for different holding times.

Overall, the reduction rate of hardness for electrically annealed samples is higher than that for salt-bath annealed samples.

## 4. Discussion

### 4.1. Microstructure

The most important microstructural changes observed during electrical annealing are twin formation and rapid restoration phenomena.

#### 4.1.1. Microstructure twins

In this research, very few numbers of twins were observed in the samples subjected to CGP. Other studies have reported the formation of deformation twins in copper [14].

The numbers of twins can be explained by the Taylor dislocation hardening model, which expresses local shear stress as follows [15]:

$$\tau = \alpha' G b \sqrt{\rho} \quad (2)$$

where  $G$  is the shear modulus,  $b$  is the magnitude of the Burgers vector,  $\rho$  is the dislocation density, and  $\alpha'$  is an experimental constant. This relation reveals that local shear

stress increases in CGP samples because of the increases in dislocations. Therefore, the critical shear stress for twin formation is supplied and the deformation mechanism changes from slip to twinning.

Deformation twins are completely removed after recrystallization and another type of twins, annealing twins, is formed. A large number of twins were formed during rapid annealing with an electrical current. These twins were also observed in the samples annealed at a salt bath, but the number of twins in the former was markedly greater than that in the latter.

Many contradictory views on the formation conditions of annealing twins have been put forward. In general, researchers argue that temperature and heating rate play substantial roles in twin formation. Some scholars have concluded that low temperatures or heating rates are the main factors resulting in increased twin formation; however, other researchers claim that high temperatures or heating rates are the main factors increasing twins [16]. These two viewpoints hint that twin formation can occur during nucleation or grain growth [16].

A theory explaining twin formation states that the phenomenon occurs during grain growth. In this theory, rapid growth leads to stacking fault defects and twin formation, which means a linear correlation exists between annealing temperatures and the quantity of twins formed (note that increases in annealing temperature mean improvements in nucleation rate) [16].

The results of this research support this theory on twin formation. Specifically, in electrically annealed samples, an independent factor, i.e., the effect of electrical current (or the athermal effect), in addition to the heating effect, leads to acceleration of the recrystallization process. In fact, vast numbers of nuclei rapidly grow in the early stages of recrystallization, leading to increases in stacking fault defects and, eventually, twin formation.

Previous reports indicate that electrical annealing decreases the number of twins formed [11,17]. This phenomenon occurs when the grain boundaries are not sharp, which means the boundary area per unit volume is large. The velocity of grain boundary movement increases accordingly, and twin boundary formation inevitably occurs in the later stages of the growth process [17]. In the current study, the microstructure images obtained indicate that the boundaries are sharp from the early stages of recrystallization; thus, the twin boundaries are enhanced.

The results of some investigations demonstrate that more twins are formed during restoration when the grain sizes are smaller [18] because annealing twins have lower energies

than high-angle grain boundaries and twin boundaries can act as barriers against grain boundary migration at high temperatures. Therefore, the presence of many twins is equivalent to a finer grain structure [18]. The presence of more twins and a finer grain structure in electrically annealed samples in comparison with those in salt-bath annealed samples confirms the preceding explanations.

#### 4.1.2. Recrystallization

The microstructural observations indicate that recrystallization during electrical annealing is rapidly completed within a few seconds (e.g., the sample annealed at 300°C for 0.5 s).

Hypotheses regarding rapid annealing and its effect on microstructure evolutions vary widely. Some researchers believe that increasing the heating rate inhibits recovery and recrystallization because of the short heating time [19]. Other scientists argue that increases in heating rate accelerate the recrystallization process. In other words, rapid heating treatment, instead of stored energy reduction by polygonization, can quickly remove statistically stored dislocations [20].

Speculations on electrical annealing are not restricted to the influence of heating rate. Many other researchers have concluded that dislocation movement, their reactions, and the rate of subgrain growth are accelerated as a result of electrical annealing [8,21–22].

When an electrical current passes through a metal, a flow of electrons is produced. Collisions between electrons and the atoms in a crystal lattice transfer energy from the former to the latter. In fact, creation of positive and negative poles, in addition to the heating effect, leads to enhancements in atom vibration during electrical annealing; by contrast, in conventional annealing, only the heating effect leads to atom vibration. Increases in atom vibration during electrical annealing cause the number of atoms crossing the lattice barrier to increase [9]. Thus, the kinetics of recrystallization also increases. These findings reveal that the intensity and rate of recrystallization are directly related to the number of passed electrons through cross section.

##### 4.1.2.1. Nucleation resulting from an electrical current

The recrystallization process of electrically annealed samples in this work is noticeably completed within a very short period of time (e.g., 0.5 s at 300°C). This observation may be explained in two aspects [20]: (1) formation of a large number of nuclei and (2) increases in the movement velocity of grain boundaries.

Comparing the microstructures of the sample electrically annealed at 300°C for 0.5 s and that of the sample annealed in salt bath at 300°C for 120 s, recrystallized grains in the electrically annealed sample appear to be smaller. Thus, ac-

celeration of the recrystallization process during electrical annealing is related to improvements in nucleation rate. This acceleration can be explained as follows:

(1) Because of the high heating rate applied in electrical annealing, recovery does not occur; thus, a larger driving force is provided to the deformed metal at high temperatures and the nucleation rate is increased.

(2) Some studies report that, during electrical annealing, temporary thermal compressive stress (owing to the effect of concentrated heat on a region in atomic scale) is the most important factor influencing enhancements in dislocation mobility directly affecting the increase in nucleation rate [23–26].

(3) Several researchers have observed that the current effect, besides the heating effect, causes reductions in thermodynamic barriers and enhancements in atomic diffusion [27–28]. In other words, in deformed metals, nucleation occurs through subgrain coalescence, which is associated with dislocation glide and climb. Electrical currents cause atom vibrations to increase and leads to acceleration of the climbing process [11]. As a result, the dislocation mobility is increased and subgrain coalescence (or the nucleation process) occurs more rapidly.

Based on classical nucleation theory, the recrystallization nucleation rate in a current-carrying system is expressed as [28]:

$$I_r^{\text{EPT}} = I_r^0 \left( \frac{D}{\lambda^2} \right) \exp \left( - \frac{\Delta G_r^0 + \Delta G_r^c}{RT} \right) \quad (3)$$

where  $I_r^0$  is a constant of the recrystallization process,  $\lambda$  is the jump distance of atoms,  $D$  is an atomic diffusion coefficient,  $\Delta G_r^0$  is the free energy change for recrystallization in a current-free system, and  $\Delta G_r^c$  is the free energy change for recrystallization in a current-carrying system. Since  $\Delta G_r^c$  is negative [28], the nucleation rate ( $I_r$ ) during electrical annealing is higher than that during conventional annealing.

##### 4.1.2.2. Gibbs free energy changes during the electrical annealing of copper

The extent of reduction of thermodynamic barriers during recrystallization is related to the metal conductivity of a sample. Copper shows obvious free energy changes because of its high electrical conductivity. The change in Gibbs free energy during electrical annealing ( $\Delta G_r^{\text{EPT}}$ ) may be considered as [10,28]:

$$\Delta G_r^{\text{EPT}} = \Delta G_r^0 + \Delta G_r^c \quad (4)$$

In this equation,  $\Delta G_r^{\text{EPT}}$  is the change of the total free energy. If the deformed metal is represented by  $\alpha_d$  and the recrystallized nucleus is represented by  $\alpha_r$ ,  $\Delta G_r^c$  can be described as [10,28]:



$$\Delta G_r^e = \mu_0 g \xi(\sigma_{\alpha_r}, \sigma_{\alpha_d}) j^2 \Delta V \quad (5)$$

where  $\mu_0$  is the magnetic susceptibility in a vacuum,  $g$  is a positive geometrical factor,  $j$  is the current density,  $\Delta V$  is the volume of a nucleus, and  $\xi(\sigma_{\alpha_r}, \sigma_{\alpha_d})$  is a term resulting from the difference between the electrical conductivity of a deformed metal ( $\alpha_d$ ) and that of a recrystallized nucleus ( $\alpha_r$ ). In Eq. (5),  $\xi(\sigma_{\alpha_r}, \sigma_{\alpha_d})$  is given by [10,28]:

$$\xi(\sigma_{\alpha_r}, \sigma_{\alpha_d}) = \frac{(\sigma_{\alpha_d} - \sigma_{\alpha_r})}{(2\sigma_{\alpha_d} + \sigma_{\alpha_r})} \quad (6)$$

where  $\sigma$  is the electrical conductivity.

$$\Delta G_r^e \propto \xi j^2, \text{ and the current density } (j) \text{ is proportional to}$$

$$j = \frac{I}{A} = \frac{(V/R)}{A} = \frac{V}{A} \sigma \rightarrow j^2 \propto \sigma_{\alpha_d}^2 \quad (7)$$

where  $I$  is the electrical current,  $A$  is the area of perpendicular cross section to the motion direction of electrons,  $V$  is the voltage, and  $R$  is the electrical resistance. Thus, from Eqs. (6) and (7):

$$\Delta G_r^e \propto \xi j^2 \rightarrow \Delta G_r^e \propto \frac{(\sigma_{\alpha_d} - \sigma_{\alpha_r})}{(2\sigma_{\alpha_d} + \sigma_{\alpha_r})} \sigma_{\alpha_d}^2 \quad (8)$$

Eq. (8) indicates that a high metal electrical conductivity translates to greater changes in Gibbs free energy. This relationship provides an explanation for the extremely rapid completion of recrystallization observed in the current study.

#### 4.1.2.3. Grain growth resulting from an electrical current

Comparison of the metallographic images of electrically annealed samples with those of samples annealed in the salt bath (under the condition of a fully recrystallized microstructure) reveals that the grain size of the former is smaller than that of the latter.

The high grain growth of the samples annealed in the salt bath is the outcome of higher boundary mobility velocities. The grain growth velocity ( $V_{GB}$ ) is described by [29]:

$$V_{GB} = mp \quad (9)$$

where  $m$  is the grain boundary mobility and  $p$  is the driving force for growth that depends on the stored energy in a material. According to Eq. (9), driving force and grain boundary mobility are two factors determining the movement velocity of grain boundaries.

Considering Eq. (9), when an electrical current passes through a material, its grain growth rate does not increase because of two main reasons [8,20]: (1) The high nucleation rate observed in electrical annealing maintains a low driving force for growth attributable to the low density of remaining dislocations. Therefore, the growth rate observed during electrical annealing is limited.

(2) Since the nucleation rate during electrical annealing is high, a large number of nuclei are formed. Rapid collision (contact of boundaries) causes grain mobility to decrease and grain growth is limited.

## 4.2. Hardness

In Fig. 10, the hardness of fully annealed sheets subjected to CGP shows a substantial increase relative to that of primary annealed sheets. Copper sheet strengthening resulting from plastic deformation is due to increases in dislocation density and grain refinement after severe straining, as reported in Ref. [12].

The fact that the hardness values of electrically annealed samples required only a few seconds to match those of the samples annealed in the salt bath indicates that recrystallization is quickly achieved by electrical annealing. Reductions in the temperature and time required to complete recrystallization by electrical annealing have been reported previously [8,22]; this behavior can be attributed to enhancements in nucleation rate.

## 4.3. Explanation for the unusual recrystallization behavior observed in electrically annealed samples

In the hardness graph (Fig. 11), an unusual behavior consistent with the microstructure images is observed. This unusual behavior can be explained by investigating thermal and athermal effects.

A relationship between changes in Gibbs free energy related to athermal effects and the square of the current density was established in Eq. (5). Therefore, to study athermal effects, the relationship between the current density and two independent parameters (time and temperature) was investigated. The law of conservation of energy without consideration of energy loss by short-term air and system clamps can be written as

$$E_1 = E_2 \rightarrow R(t)I^2(t)dt = mC_p dT \quad (10)$$

where  $E$  is energy,  $R$  is the electrical resistance,  $m$  is the mass,  $C_p$  is the specific heat capacity,  $t$  is the time, and  $T$  is the temperature. If, in Eq. (10), instead of AC current, the root mean square current ( $I_e$ ) is substituted, the following equation is obtained (because the system voltage remains constant and the current is considered constant ( $I_e$ ), electrical resistivity changes are not taken into account):

$$RI_e^2 dt = mC_p dT \quad (11)$$

If Eq. (11) is divided by the square of the cross sectional area:

$$Rj_e^2 dt = \frac{mC_p dT}{A^2} \quad (12)$$

Eq. (12) indicates that  $j^2 \propto \frac{dT}{dt}$  ( $j^2 = j_e^2$ ). If  $\Delta G_r^e \propto j^2$  (Eq. (5)), then  $\Delta G_r^e \propto \frac{dT}{dt}$ . This relationship allows the simultaneous investigation of the influences of heat and electrical current on the recrystallization process.

When the heating time is held constant, both thermal and athermal effects increase as a result of increases in temperature. Consequently, the fraction of recrystallized grains also increases. This behavior is similar to observations made during conventional annealing and consistent with the remaining findings of the current research.

When the maximum temperature is held constant, a negatively linear correlation is observed between thermal and athermal effects as the heating time is increased. Increases in heating time increase thermal effects but decrease athermal effects because of the reduction in heating rate and the relationship obtained in Eq. (12). Therefore, conflict between thermal and athermal effects determines the recrystallized fraction, and the unusual behavior of the samples electrically annealed at 150 and 200°C may be explained by the contradictory effects of the time parameter.

## 5. Conclusions

(1) Electrically annealed samples appear to form more numbers of twins than conventionally annealed samples. These twins are formed during grain growth because the rapid growth of grains leads to stacking fault defects.

(2) The recrystallization process in electrically annealed samples is completed within a very short period of time (e.g., samples electrically annealed at 250 and 300°C for 0.5 s). Acceleration of the recrystallization process is related to increases in nucleation rate during annealing. In other words, improvements in atomic diffusion resulted from both thermal and athermal effects lead to enhancements in dislocation climb velocity and subgrain coalescence. The nucleation rate and kinetics of recrystallization increase accordingly.

(3) Electrical annealing does not accelerate the grain growth process. In this case, the nucleation rate decreases the driving force for grain growth and reduces the mobility of grain boundaries due to rapid collisions among boundaries.

(4) The microstructural observations and hardness results of the samples electrically annealed up to 150 and 200°C illustrate that, unlike conventional annealing, electrical annealing at a constant temperature with increasing heating time does not necessarily result in reductions in hardness

because of conflicts between thermal and athermal effects.

## Acknowledgements

The authors wish to thank the research board of Sharif University of Technology for the financial support and the provision of the research facilities used in this work.

## References

- [1] M. Atkinson, On the credibility of ultra-rapid annealing, *Mater. Sci. Eng. A*, 354(2003), No. 1-2, p. 40.
- [2] J. Wang, J. Li, X.F. Wang, J.J. Tian, C.H. Zhang, and S.G. Zhang, Effect of heating rate on microstructure evolution and magnetic properties of cold rolled non-oriented electrical steel, *J. Iron Steel Res. Int.*, 17(2010), No. 11, p. 54.
- [3] A.A. Gazder, V.Q. Vu, A.A. Salah, P.E. Markovskiy, O.M. Ivashin, C.H.J. Davies, and E.V. Pereloma, Recrystallisation in a cold drawn low cost beta titanium alloy during rapid resistance heating, *J. Alloys Compd.*, 585(2014), p. 245
- [4] F. Lefevre-Schlick, X. Wang, and D. Embury, The production of fine-scale microstructures by rapid annealing, *Mater. Sci. Eng. A*, 483-484(2008), p. 258.
- [5] R.F. Zhu, G.Y. Tang, S.Q. Shi, and M.W. Fu, Microstructure evolution of copper strips with gradient temperature in electropulsing treatment, *J. Alloys Compd.*, 581(2013), p. 160.
- [6] W. Zhang, M.L. Sui, Y.Z. Zhou, and D.X. Li, Evolution of microstructures in materials induced by electropulsing, *Micron*, 34(2003), No. 3-5, p. 189.
- [7] Y.H. Zhu, S. To, W.B. Lee, X.M. Liu, Y.B. Jiang, and G.Y. Tang, Effects of dynamic electropulsing on microstructure and elongation of a Zn–Al alloy, *Mater. Sci. Eng. A*, 501(2009), No. 1-2, p. 125.
- [8] Y.B. Jiang, G.Y. Tang, C.H. Shek, J.X. Xie, Z.H. Xu, and Z.H. Zhang, Mechanism of electropulsing induced recrystallization in a cold-rolled Mg–9Al–1Zn alloy, *J. Alloys Compd.*, 536(2012), p. 94.
- [9] W.C. Wu, Y.J. Wang, J.B. Wang, and S.M. Wei, Effect of electrical pulse on the precipitates and material strength of 2024 aluminum alloy, *Mater. Sci. Eng. A*, 608(2014), p. 190.
- [10] W. Jin, J.F. Fan, H. Zhang, Y. Liu, H.B. Dong, and B.S. Xu, Microstructure, mechanical properties and static recrystallization behavior of the rolled ZK60 magnesium alloy sheets processed by electropulsing treatment, *J. Alloys Compd.*, 646(2015), p. 1.
- [11] Z.H. Xu, G.Y. Tang, S.Q. Tian, and J.C. He, Research on the engineering application of multiple pulses treatment for recrystallization of fine copper wire, *Mater. Sci. Eng. A*, 424(2006), No. 1-2, p. 300.
- [12] E. Rafizadeh, A. Mani, and M. Kazeminezhad, The effects of intermediate and post-annealing phenomena on the mechanical properties and microstructure of constrained groove pressed copper sheet, *Mater. Sci. Eng. A*, 515(2009), No. 1-2, p. 162.

- [13] M.A. Mostafaei and M. Kazeminezhad, Microstructure and mechanical properties improvement by ultra-rapid annealing of severely deformed low-carbon steel, *Mater. Sci. Eng. A*, 655(2016), p. 229.
- [14] A. Kauffmann, J. Freudenberger, H. Klauß, W. Schillinger, V. Subramanya Sarma, and L. Schultz, Efficiency of the refinement by deformation twinning in wire drawn single phase copper alloys, *Mater. Sci. Eng. A*, 624(2015), p. 71.
- [15] F. Shen, J.Q. Zhou, Y.G. Liu, R.T. Zhu, S. Zhang, and Y. Wang, Deformation twinning mechanism and its effects on the mechanical behaviors of ultrafine grained and nanocrystalline copper, *Comput. Mater. Sci.*, 49(2010), No. 2, p. 226.
- [16] J.L. Bair, S.L. Hatch, and D.P. Field, Formation of annealing twin boundaries in nickel, *Scripta Mater.*, 81(2014), p. 52.
- [17] H. Conrad, N. Karam, and S. Mannan, Effect of electric current pulse on the recrystallization of copper, *Scripta Metall.*, 17(1983), No. 3, p. 411.
- [18] T.H. Chuang, C.H. Tsai, H.C. Wang, C.C. Chang, C.H. Chuang, J.D. Lee, and H.H. Tsai, Effects of annealing twins on the grain growth and mechanical properties of Ag–8Au–3Pd bonding wires, *J. Electron. Mater.*, 41(2012), No. 11, p. 3215.
- [19] F. Fang, Y.B. Xu, Y.X. Zhang, Y. Wang, X. Lu, R.D.K. Misra, and G.D. Wang, Evolution of recrystallization microstructure and texture during rapid annealing in strip-cast non-oriented electrical steels, *J. Magn. Magn. Mater.*, 381(2015), p. 433.
- [20] M. Ferry and D. Jones, High-rate annealing of single-phase and particle-containing aluminium alloys, *Scripta Mater.*, 38(1998), No. 2, p. 177.
- [21] C. Yan, N. Li, H.W. Jiang, D.Z. Wang, and L. Liu, Effect of electropulsing on deformation behavior, texture and microstructure of 5A02 aluminum alloy during uniaxial tension, *Mater. Sci. Eng. A*, 638(2015), p. 69.
- [22] G.L. Hu, Y.H. Zhu, G.Y. Tang, C.H. Shek, and J.N. Liu, Effect of electropulsing on recrystallization and mechanical properties of silicon steel strips, *J. Mater. Sci. Technol.*, 27(2011), No. 11, p. 1034.
- [23] Y.Z. Zhou, S.H. Xiao, and J.D. Guo, Recrystallized microstructure in cold worked brass produced by electropulsing treatment, *Mater. Lett.*, 58(2004), No. 12-13, p. 1948.
- [24] S.H. Xiao, J.D. Guo, S.D. Wu, G.H. He, and S.X. Li, Recrystallization in fatigued copper single crystal under electropulsing, *Scripta Mater.*, 46(2002), No. 1, p. 1.
- [25] Z.J. Wang and H. Song, Effect of electropulsing on anisotropy behaviour of cold-rolled commercially pure titanium sheet, *Trans. Nonferrous Met. Soc. China*, 19(2009), Suppl. 2, p. s409.
- [26] S.H. Xiao, Y.Z. Zhou, J.D. Guo, S.D. Wu, G. Yao, S.X. Li, G.H. He, and B.L. Zhou, The effect of high current pulsing on persistent slip bands in fatigued copper single crystals, *Mater. Sci. Eng. A*, 332(2002), No. 1-2, p. 351.
- [27] Y.Z. Zhou, W. Zhang, B.Q. Wang, and J.D. Guo, Ultrafine-grained microstructure in a Cu–Zn alloy produced by electropulsing treatment, *J. Mater. Res.*, 18(2003), No. 8, p. 1991.
- [28] X.X. Ye, Z.T.H. Tse, G.Y. Tang, X.H. Li, and G.L. Song, Effect of electropulsing treatment on microstructure and mechanical properties of cold-rolled pure titanium strips, *J. Mater. Process. Technol.*, 222(2015), p. 27.
- [29] F.J. Humphreys and M. Hatherly, *Recrystallization and Related Annealing Phenomena*, 2nd Ed., Elsevier, Oxford, 2004, p. 219.